Journal of Neuropathology and Experimental Neurology

Vol. 56, No. 8
August, 1997
pp. 901–911

Glutamate Transporter Alterations in Alzheimer Disease Are Possibly Associated with Abnormal APP Expression

SHI LI, PHD, MARGARET MALLORY, BS, MICHAEL ALFORD, BA, SEIGO TANAKA, PHD, AND ELIEZER MASLIAH, MD

Abstract. Recent studies have shown that deficient functioning of glutamate transporters (GTs) in Alzheimer disease (AD) might lead to neurodegeneration. The main objectives of the present study were to determine which GT subtype is most affected in AD and to asses to what extent altered GT function is associated with abnormal amyloid precursor protein (APP) expression. While EAAT2-immunoreactivity (IR) was decreased in AD frontal cortex, EAAT1- and EAAT3-IR were unaffected; mRNA levels for all 3 GTs were not affected. Decreased EAAT2-IR was associated with decreased GT activity. EAAT2-IR inversely correlated with EAAT2 mRNA levels, suggesting that in AD, GT expression alterations occur due to disturbance at the post-transcriptional level. EAAT2-IR was inversely correlated with APP770 mRNA. In addition, GT activity directly correlated with APP695 mRNA and total APP protein levels, and inversely correlated with APP751/770 mRNA levels. This study supports the notion that astroglial EAAT2 is affected in AD and abnormal functioning and/or processing of APP might play an important role in this process.

Key Words: Alzheimer disease; Amyloid precursor protein; Excitotoxicity; Glutamate transporter; Neurodegeneration.

INTRODUCTION

Glutamate is the predominant excitatory neurotransmitter in the mammalian central nervous system (CNS) (1). Glutamate is normally cleared from the synaptic cleft by high-affinity, Na^+-dependent uptake transporters located in both neurons and glia (1–3). Recently, at least 4 high-affinity, Na^+-dependent uptake carriers of aspartate/glutamate (also known as glutamate transporters [GTs]) have been cloned: (a) EAAT1 (or GLAST) (4), (b) EAAT2 (or GLT-1) (5), EAAT3 (or EAAC1) (6), and the cerebellar transporter EAAT4 (7). These transporters exhibit 39 to 55% sequence homology with each other (7). EAAT1 is localized in subsets of neurons and glial cells (8), EAAT2 is specifically located in astrocytes, and EAAT3 has a neuronal localization that includes nonglutaminergic neurons. Glutamate transporters are also thought to be critical in preventing excessive extracellular accumulation of this potentially neurotoxic chemical (1–3, 9). Several lines of evidence suggest that inefficient glutamate transport leads to accumulation of excessive neurotransmitter in the synapse, resulting in subsequent neurotoxicity. Experimentally induced pharmacological or molecular blockade of GTs causes neuronal death in both acute and chronic models (9, 10). Furthermore, in amyotrophic lateral sclerosis (ALS) there is selective loss of the glial GT (type EAAT2) (11) in the motor cortex. In Alzheimer disease (AD), the high affinity glutamate/aspartate uptake system is 40 to 50% decreased in the frontal, parietal and temporal cortex (12–14). In addition, recent studies have shown that in AD, increased levels of brain spectrin degradation products (marker of calpain I activation and excitotoxicity) were correlated with a decrease in the levels of D- and L- [^{3}H]aspartate binding (marker of GT activity) and decreased levels of synaptophysin immunoreactivity (SYN-IR) (general presynaptic terminal marker) (15). Furthermore, the levels of L-[^{3}H]aspartate uptake were directly correlated with SYN-IR and inversely correlated with the Blessed score. Taken together, these results suggest that decreased activity of the glutamate transporters in AD is associated with increased excitotoxicity and neurodegeneration, and supports the possibility that abnormal functioning of this system might be involved in the pathogenesis of the synaptic damage in AD (15).

The factors involved in regulating the function of the GT that might be affected in AD are not clearly known yet; furthermore, it is also not clear which GT is more selectively affected. Previous studies have shown that amyloid precursor protein (APP) protects against excitotoxicity (16–18). It has been postulated that secreted APP (sAPP) might prevent the toxicity associated with stimulation of glutamate receptors by stabilizing intracellular Ca^{2+} levels (16, 19, 20) through a mechanism that involves activation of K+ channels (21). More recently, studies in transgenic mice have shown that APP overexpression might protect against excitotoxicity by enhancing GT functioning (22). Therefore, abnormal functioning of sAPP may be involved in the mechanisms of synaptic damage in AD by failing to promote or maintain the normal levels of glutamate at the synaptic cleft (15). In this context, the main objectives of the present study were to (a) determine which GT is more specifically affected in AD, and (b) assess to what extent altered

From the University of California, San Diego, School of Medicine, Departments of Neurosciences (MM, MA, ST, EM) and Pathology (EM), La Jolla, CA 92093-0624.

Correspondence to: Dr E. Masliah, Department of Neurosciences, University of California, San Diego, La Jolla, CA 92093-0624.

Sources of support: This work was supported by NIH/NIA Grants AG10689 and AG05131 and by Grants from the Alzheimer's Disease and Related Disorders Association, Inc. and the American Federation for Aging Research.

TABLE 1
Summary of Clinical, Pathological and Neurochemical Findings

Group	n	Age	PMT	Midfrontal total plaques	Midfrontal neuritic plaques	Midfrontal tangles	Blessed score	L-aspartate	D-aspartate
Control	4	76.5 ± 6	5 ± 2	0	0	0	0	262.2 ± 17.21	286.0 ± 41.5
Alzheimer disease	12	79.6 ± 2.5	8 ± 4	42.4 ± 3.8**	33.8 ± 4.5**	2.58 ± 1.04*	18.9 ± 3.7*	169.3 ± 25.2*	174.0 ± 19*

* $p < 0.05$ (Student's t-test, unpaired, two-tailed). ** $p < 0.01$ (Student's t-test, unpaired, two-tailed).

GT function is associated with abnormal APP expression. For this purpose, levels of 3 different GTs at the mRNA, protein and activity levels were measured in the frontal cortex of AD cases and correlated with neuropathological and clinical markers of the disease, as well as with levels of APP.

MATERIALS AND METHODS

Samples and Neuropathological Assessment

Sixteen autopsy cases from the Alzheimer Disease Research Center at the University of California, San Diego, were included for the present analysis. Table 1 summarizes the clinical and neuropathological characteristics of the cases included for this study. In all cases detailed neuropathological and clinical data was available and tissue available for examination showed a good RNA preservation (23). Furthermore, in all of these cases material was available for immunocytochemical and Western blot analysis and D- and L- [^{3}H]aspartate uptake. Twelve of the cases had clinical histories of AD, confirmed at autopsy. The average age of the AD cases was 79.6 ± 2.5 years, with a postmortem delay of 8 ± 4 hours (h). Two of these cases died of pneumonia, 4 died of myocardial infarction, and 6 died of cardiorespiratory arrest. The 4 control cases were clinically and histopathologically free of neurological disease. The average age of this control group was 76.5 ± 6 years with a postmortem delay of 5 ± 2 h. The causes of death in these cases were pneumonia, lung cancer, emphysema, and cardiac arrest. As we have previously shown, these perimortem conditions did not significantly alter the quality of the RNA obtained (23). Blocks from the frontal cortex and posterior hippocampus were fixed in 2% buffered paraformaldehyde for 72 h at 4°C and serially sectioned at 40 μm with the Vibratome 2000 (Technical Products International, Inc., St. Louis, MO). Paraffin sections from cortical and subcortical regions were stained with hematoxylin and eosin, Thioflavine-S and Cresyl violet for routine histopathological examination and morphometric analysis, as previously described (24).

Generation of Riboprobes for Glutamate Transporters

DNA templates for GT riboprobes were generated from total RNA extracted from human mid-frontal cortex by reverse transcriptase polymerase chain reaction (RT-PCR). Cyclophilin template was obtained from Ambion (Austin, TX). Reverse transcriptase reactions were performed in 20 μl 1 × first strand buffer (Life Technologies, Inc.) with 3 μg RNA, 250 ng random hexamers, 0.5 mM dNTP mix, 20 unit RNasin, 10 mM DTT and 100 units of Malony murine leukemia virus reverse transcriptase (Life Technologies, Inc.). The reaction mixtures were incubated sequentially at room temperature (10 min), 37°C (30 min) and 95°C (5 min). For PCR, 30 cycles of denaturation (45 seconds, 94°C), annealing (1 min, 48°C), and extension (1 min, 72°C) were performed in 50 μl reactions that contained 0.5 μM of each primer, 2 μl of RT reaction, 200 μM dNTP mix, 2.5 units of Taq and 1 × PCR buffer (Boehringer-Mannheim, Indianapolis, IN). Three pairs of oligonucleotide primers (23 to 28 mers) complementary to human GT genes were used to amplify DNA templates complementary to the following sequences (GenBank accession numbers in parenthesis): nucleotides 1544–1661 (U03504) of EAAT1; nucleotides 1644–1872 (U01824) of EAAT2; and nucleotides 1577–1740 (U08989) of EAAT3. Each primer contained EcoRI or BamHI restriction site at 5' for amplification product cloning in pGEM-7zf (Promega).

^{32}P-labeled antisense riboprobes were generated from linearized plasmids with SP6 Riboprobe® in vitro transcription system (Promega). Certain probes were labeled to lower specific activities due to relative abundance. On average, the specific activities were as follows: EAAT1 (1.3 × 108 cpm/μg), EAAT2 (6.6 × 107 cpm/μg), EAAT3 (4.5 × 108 cpm/μg), and cyclophilin (4.0 × 107 cpm/μg).

Glutamate Transporter RNA Analysis and PhosphorImager Quantitation

Total RNA was isolated from snap-frozen tissues using Ultraspec® RNA Isolation System (Biotex Laboratories, Inc.). The quality of RNA from human postmortem tissues was assessed by electrophoresis on agarose/formaldehyde gels, Northern blotting, and densitometric comparisons of 28S and 18S ribosomal RNA bands (23). Levels of specific RNAs were determined using the RPA assay as described (23), with 5 to 30 μg total RNA. Some reactions were performed under longer digestion time and/or more RNase T2. Samples were separated on 5% acrylamide/8 M urea TBE gels and dried gels were exposed to Kodak XAR film (Eastman Kodak Co.). The data for each sample were repeated at least once. Probe-specific signals were quantitated using PhosphorImager SF and ImageQuant software (Molecular Dynamics, Sunnyvale, CA). The cyclophilin signal was used as internal standard to correct for loading differences. For comparisons of signals representing distinct probes, readings were corrected for the differences of specific activities and the number of cytosine nucleotides contained in each fragment.

Levels and Alternative Splicing of APP Transcripts by RT-PCR

The proportion of APP695, 751 and 770 mRNAs in the frontal cortex of control and AD cases was determined by RT-PCR. As for the RPA, special attention was paid to verify RNA quality. Total RNA (500 ng), suspended in 12 μl DEPC-treated water with 15 pmol RT primer, was heated at 65°C for 15 min and immediately cooled on ice. To this solution a mixture of 4 μl of 5× first strand buffer (250 mM Tris-HCl [pH 8.3], 375 mM KCl, and 15 mM $MgCl_2$) was added, 1 μl of 10 mM each dNTP mixture, 2 μl of 0.1 M dithiothreitol, and 1 μl (200 units) of moloney murine leukemia virus (M-MLV) reverse transcriptase (Bethesda Research Laboratories). This reaction mixture was incubated at 42°C for 1 h to synthesize complementary DNA (cDNA).

The 20 pmol of forward primer for PCR was incubated at 37°C for 10 min with 40 units of T4 polynucleotide kinase (BRL) in 100 μl of the reaction mixture (70 mM Tris-HCl [pH 7.6], 10mM $MgCl_2$, 100 mM KCl, and 1 mM 2-mercaptoethanol) containing 10 μl (33.3 pmol) of [γ-^{32}P]ATP (10 μCi/μl, 3000 Ci/mmol). PCR amplification was performed with 1.5 units of Taq polymerase (Bethesda Research) in 50 μl of 1× PCR buffer (20 mM Tris-HCl [pH 8.4], 50 mM KCl), containing 0.2 mM each dNTP mixture, 1.5 mM $MgCl_2$, 15 pmol each of forward and reverse primers, and 1 pmol of ^{32}P-labeled forward primer.

Sequence of the RT primer was TTGGCTGCTTCCTGTTCCA complementary to the sequence 1118–1100 of APP695 cDNA; that of the forward primer for PCR was GCCAAAGAGACATGCAG corresponding to sequence 460–476; and that of the reverse primer was TCTCCTGGAAATGCTGG complementary to the sequence 1071–1087. The thermal cycle profile was as follows: (a) denaturation at 94°C for 30 sec, (b) annealing at 47°C for 1 min, and (b) extension at 72°C for 40 sec. The amplification was done for various cycle numbers (19, 21, 23, 25, 27 and 29).

Ten μl of each PCR reaction mixture was electrophoresed in 3.5% polyacrylamide gel. Gels were dried and autoradiographed. Dried gels were also scanned by PhosphorImager (Molecular Dynamics) and quantitative analysis was carried out using ImageQuant (Molecular Dynamics).

Antibodies

The polyclonal antibodies against GTs were generated at Research Genetics Inc. (Huntsville, AL) with synthetic peptides corresponding to the C-terminal region of the EAAT1, EAAT2 and EAAT3 proteins. An N-terminal lysine was added to the peptides to facilitate coupling to the carrier. The sequences of the peptides selected to generate the antibodies were based on work previously published by Rothstein et al (8). The crude antisera were generated against KLH-conjugated synthetic peptides in rabbits and affinity purified. The mouse monoclonal antibody against APP (8E5, courtesy of Athena Neurosciences Inc., San Francisco, CA) was used for Western blot analyses, as previously described (17, 18). This antibody was generated with APP residues 444-592 and specifically recognizes human APP. In addition, mouse monoclonal antibodies against the synaptic marker-SYN (SY38, Boehringer-Mannheim, Indianapolis, IN) (25,26), amyloid ß/A4 (clone 3D6, generated with amyloid peptide 1–6, Athena Neurosciences Inc., San Francisco, CA), and the astroglial marker-glial fibrillary acidic protein (GFAP, Boehringer) were used for double-immunocytochemical analyses.

Determination of GT and Human APP (hAPP) IR Levels by Western Blot

Western blot analysis was performed as previously described to estimate the levels of EAAT1- EAAT2-, EAAT3- and hAPP-IR. For GTs the rabbit polyclonal antisera (0.25 μg/ml) generated with synthetic peptides was used; for confirmation of levels of hAPP-IR the mouse monoclonal antibody 8E5 (0.1 μg/ml) (17) was used.

Aliquots from the neocortical brain homogenates were separated into cytosolic and particulate fractions as previously described (27, 28). To assure equal loading, the protein content of all samples was determined by Lowry assay (29) and adjusted with homogenization buffer to 1.25 mg/ml; 40 μg of brain protein were loaded per lane. Briefly (27), samples from the particulate fractions were loaded into 10% SDS-polyacrylamide gels, electrophoresed and blotted onto nitrocellulose paper. Control and AD samples from all 16 cases were run in the same gel to assure reproducibility of results. Blots were incubated with blocking solution followed by the anti-primary antibody. Radio-iodinated protein A (ICN, Irvine, CA) bound to secondary antibodies (for primary mouse monoclonal) were detected using a PhosphorImager SF (Molecular Dynamics). Signals were quantified by integrating pixel intensities over defined volumes using the ImageQuant software (27). Since previous studies have shown (30) that for APP the triplet band at an estimated MW of 110-120 kDa might not necessarily correspond to the 3 major transcripts, but rather to post-transcriptional modifications, we did not attempt to quantify each individual band using the ImageQuant software. Instead, we estimated the levels of IR of the triplet as a whole. Determinations of APP transcript levels were done by RT-PCR, as described in the previous section. Control experiments were performed by incubating similar blots containing homogenates from control and AD cases with preimmune sera or with the antibody preadsorbed with 20-fold excess of the corresponding specific peptide.

Evaluation of Expression Levels and Distribution of GT by Immunocytochemistry

Analysis of the patterns of immunolabeling and distribution of GTs in AD and control brains was carried out by immunostaining vibratomed sections, as previously described (31), with rabbit polyclonal antibodies against GTs—EAAT1, EAAT2 and EAAT3 (0.5 μg/ml). Further verification of antibody specificity was done by incubating tissue sections with the antibody preadsorbed with 20-fold excess peptide and/or with preimmune sera. Briefly, vibratome sections from the midfrontal cortex and posterior hippocampus were first washed in PBS (pH 7.4), blocked with 10% normal serum, and incubated overnight at 4°C with the primary antibody. The free-floating sections were then washed in PBS and incubated with the biotinylated anti-goat secondary antibody made in rabbit (Vector, Burlingame, CA), followed by Avidin D-HRP (ABC Elite, Vector), and reacted with diaminobenzidine tetrahydrochloride (DAB, 0.2 mg/ml) in 50 mM Tris buffer (pH 7.4) with 0.001% hydrogen peroxide.

All sections were run simultaneously and under identical conditions to assure reproducibility of the results. Immunolabeled sections were analyzed with the Quantimet 570C microdensitometer, as previously described, in order to semiquantitatively determine the levels of immunoreactivity (corrected optical density) (27, 32, 33). Since the white matter also shows GT immunoreactive cells, correction for background was done by subtracting the optical density of adjacent sections immunostained with the preimmune sera.

Double Immunolabeling and Laser Confocal Imaging

In order to asses the relationship between amyloid deposition, neurodegeneration and GT expression, 40-μm-thick vibratome sections from control and AD cortex were double-immunolabeled (34) with the following combinations of monoclonal/polyclonal antibodies: (a) GFAP/EAAT2, (b) amyloid ß/A4 (3D6)/EAAT2, (c) SYN/EAAT2, and (d) SYN/EAAT3. Sections were then incubated with the goat anti-rabbit biotinylated antibody (1:100, Vector) followed by a mixture of FITC-conjugated horse anti-mouse IgG (1:75, Vector) and Texas Red Avidin D (1:150) (Jackson ImmunoResearch Labs, West Grove, PA). The double-labeled sections were transferred to SuperFrost slides (Fisher Scientific, Tustin, CA) and mounted under glass coverslips with anti-fading media (Vector). The sections were studied with the Bio-Rad MRC-1024 laser scanning confocal microscope (34) mounted on an Axiovert Zeiss microscope. This system permits the simultaneous analysis of double-immunolabeled samples in the same optical plane.

Serial optical sections, 0.5 μm thick, of the neocortex displaying the GTs were recorded in the FITC channel, and the corresponding serial images of anti-amyloid ß/A4, SYN and GFAP were recorded in the Texas red channel. The aperture, contrast and gain level were initially adjusted manually to obtain images with a pixel intensity within a linear range. For each case and condition, a total of 20 fields were imaged. These digitized images were used to determine the proportion of EAAT2-positive cells that were also GFAP-positive inside and outside of the plaques, and the proportion of diffuse and mature plaques (3D6 immunostained) that were EAAT2-immunoreactive.

D- and L-[^{3}H] Aspartate Binding Assay

In order to estimate GT activity, D- and L- [^{3}H]aspartate binding assay was performed on washed membrane preparations by a modified method of Cross et al (35). As previously described (15), frozen samples (approximately 100 mg wet weight) from the midfrontal cortex of control and AD cases were sonicated in 1 ml 50 mM Tris-HCl/300 mM NaCl buffer, pH 7.4. Nine additional mls of buffer were added followed by centrifugation at 21,780 × g for 30 minutes (min) at 4°C. The supernatant was decanted and the pellet resuspended in 10 mls buffer. Total protein was determined by the method of Lowry (29). Samples were diluted to 0.4 mg/ml total protein. One ml incubation volumes in triplicate tubes containing 40 μg (100 μl) of washed membranes and a final concentration of 50 nM D- or L- [^{3}H]aspartate (Dupont NEN Research Products, Boston MA) and 4000 nM unlabeled (cold) aspartate were incubated at room temperature for 30 min. Nonspecific binding was determined by adding 10-fold excess (40,000 nM) cold aspartate to otherwise identical incubation tubes. Membranes and unbound ligand were separated by rapid filtration through 0.45 μ glass fiber filters on a disposable filtration manifold (V&P Scientific, San Diego, CA), followed by 2 × 200 μl washes of 50 mM Tris HCl/300mM NaCl buffer. Filter disks were counted in 7 ml vials containing 5 ml EcoLume scintillation cocktail (ICN) on a TM Analytic 6881 Mark III scintillation spectrophotometer. Results were expressed as pMol bound per mg total protein.

Statistical Analyses

All samples were assigned a blind code before initiating the experiments. The code was broken after all the results were downloaded into the database. Statistical analysis was performed utilizing the StatView program running on a Macintosh 6100/66. Differences between control and AD were tested using the unpaired, two-tailed Student's t test. The relationship between 2 specific variables was tested using the Pearson product-moment correlation, r value, calculated with simple linear regression analysis. To avoid artificial skewing of regression line by control cases, only AD cases were included for this analysis. Results were expressed as mean +/- SEM.

RESULTS

Levels of GT mRNA Expression in the AD Frontal Cortex

Levels of mRNA expression for the 3 different GT subtypes were assessed by RNase protection assay (RPA) in the frontal cortex of control and AD cases. The probe for EAAT1 protected a band at 121 bp (Fig. 1b), the EAAT2 probe protected a band at 229 bp (Fig. 1a), and the one for EAAT3 a band at 164 bp (Fig. 1b). The astroglia-specific transporter EAAT2 showed the highest expression level (Fig. 1a), followed by EAAT1 (75% of EAAT2 level) (Fig. 1b) and the neuron-specific EAAT3 (about 5% of EAAT2 level) (Fig. 1b). In other areas of the brain (such as hippocampus and cerebellum), the ratios of various transporter expression were similar to the frontal cortex (data not shown). Compared with controls, AD cases showed a slight trend toward increased levels of EAAT2 mRNA in the frontal cortex; however, this difference was not statistically significant (Fig. 1c). Furthermore, no significant differences in the levels of EAAT1 and EAAT3 mRNA expression were observed between AD cases and controls (Fig. 1d, e).

Levels of GT-IR in the Cortex in AD

The antibody against EAAT2 recognized a major band at an estimated MW of 75 kDa (Fig. 2a), while EAAT1 recognized a major band at 65 kDa (Fig. 2b). The antibody against EAAT3 labeled 4 broad bands; the most apparent was the band at 69 kDa (Fig. 2c). In control experiments, where primary antibody was adsorbed with excess peptide, the specific bands were not labeled (Fig. 3). Furthermore, the preimmune serum did not recognize the major specific bands (Fig. 3). When compared with controls, AD cases showed a significant 30% decrease in

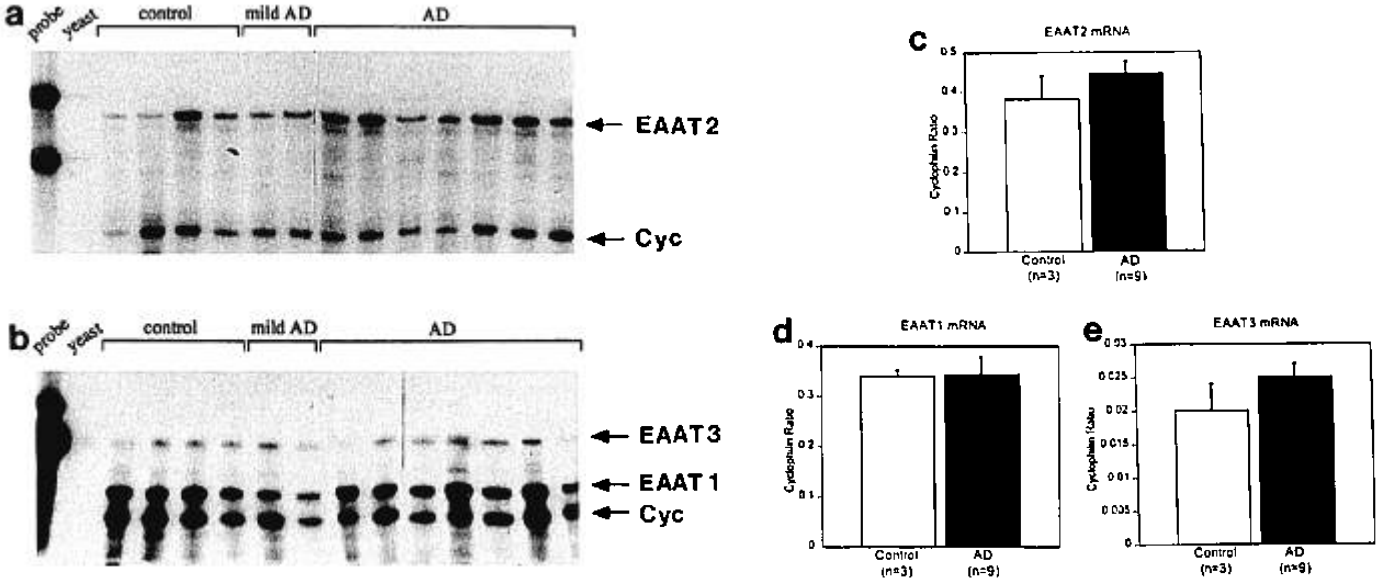

Fig. 1. Levels of GT mRNA expression in the frontal cortex by RPA. (a) The probe for the astroglia-specific transporter EAAT2 protected a band at 229 bp. (b) The probe for EAAT1 protected a band at 121 bp and the one for the neuron-specific EAAT3 a band at 164 bp. (c) Compared with controls, AD cases showed a slight trend (nonsignificant) toward increased levels of EAAT2 mRNA in the frontal cortex. (d, e) No significant differences in the levels of EAAT1 and EAAT3 mRNA expression were observed between AD and control cases.

levels of EAAT2-IR in the frontal cortex (Fig. 2d). No significant differences in levels of EAAT1-IR (Fig. 2e) and EAAT3-IR (Fig. 2f) were observed between AD and control cases.

Cellular Distribution of GT in AD

In control cases, EAAT2-IR was mainly associated with glial cells that possessed abundant processes in the frontal cortex (Fig. 4a) and hippocampus (Fig. 4b). These processes were often distributed around presynaptic terminals and dendritic branches. Double immunolabeling studies showed that EAAT2-immunoreactive cells in the neocortex often displayed anti-GFAP-IR (Fig. 5a, b). In AD cases, EAAT2-IR was also associated with glial cells in the neocortex (Fig. 4c) and hippocampus (Fig. 4d); however, these cells displayed a decrease in the intensity of immunolabeling when compared with controls. Double labeling studies showed that EAAT2-IR was colocalized with the GFAP-immunoreactive glial cells (Fig. 5c, d) surrounding the amyloid plaques, as well as with a fine meshwork of astroglial processes embedded in the amyloid core (Fig. 5e–h). EAAT2-IR was observed in approximately 30% of the plaque-containing dense amyloid core and in approximately 80% of the diffuse plaques.

In the control cases, the antibody against EAAT1 mildly immunolabeled pyramidal and glial cells (not shown). Mild EAAT3-IR was observed in the neuropil and in some pyramidal cell bodies. Double labeling studies showed that the EAAT3 immunostaining in the neuropil was associated with punctuate structures adjacent to the SYN-immunoreactive presynaptic terminals (not shown). These structures also showed microtubule-associated protein 2 (MAP2)-IR, indicating that they correspond to dendritic arbor (not shown). In AD, similar patterns of EAAT1- and EAAT3- IR were observed when compared with controls.

Correlations Among GT, mRNA Levels, IR (by Western Blot) and Binding

Consistent with previous studies (15), levels of GT activity, as assessed by D- and L- [^{3}H]aspartate binding, were decreased in the frontal cortex of the AD cases (Table 1). In order to asses the relationship among mRNA levels, IR and binding linear regression analysis was performed. This analysis showed an inverse correlation between EAAT2 mRNA and IR ($r = -0.726$, $n = 12$, $p = 0.0075$) (Fig. 6a). No significant correlations were observed between mRNA and EAAT1 or EAAT3. Furthermore, L-[^{3}H]aspartate showed a trend toward inverse correlation with EAAT1 ($r = -0.517$, $n = 11$, $p = 0.103$) and EAAT3 ($r = -0.412$, $n = 11$, $p = 0.207$) mRNA levels; however, none of these correlations were statistically significant. As for the GT-IR, the strongest correlations were observed between L-[^{3}H]aspartate binding and EAAT3 ($r = 0.613$, $n = 14$, $p = 0.0198$) and between D-[^{3}H]aspartate binding and EAAT2 ($r = 0.54$, $n = 14$, $p = 0.04$) (Fig. 6b). No significant correlations were observed between levels of GT mRNA and D-[^{3}H]aspartate binding.

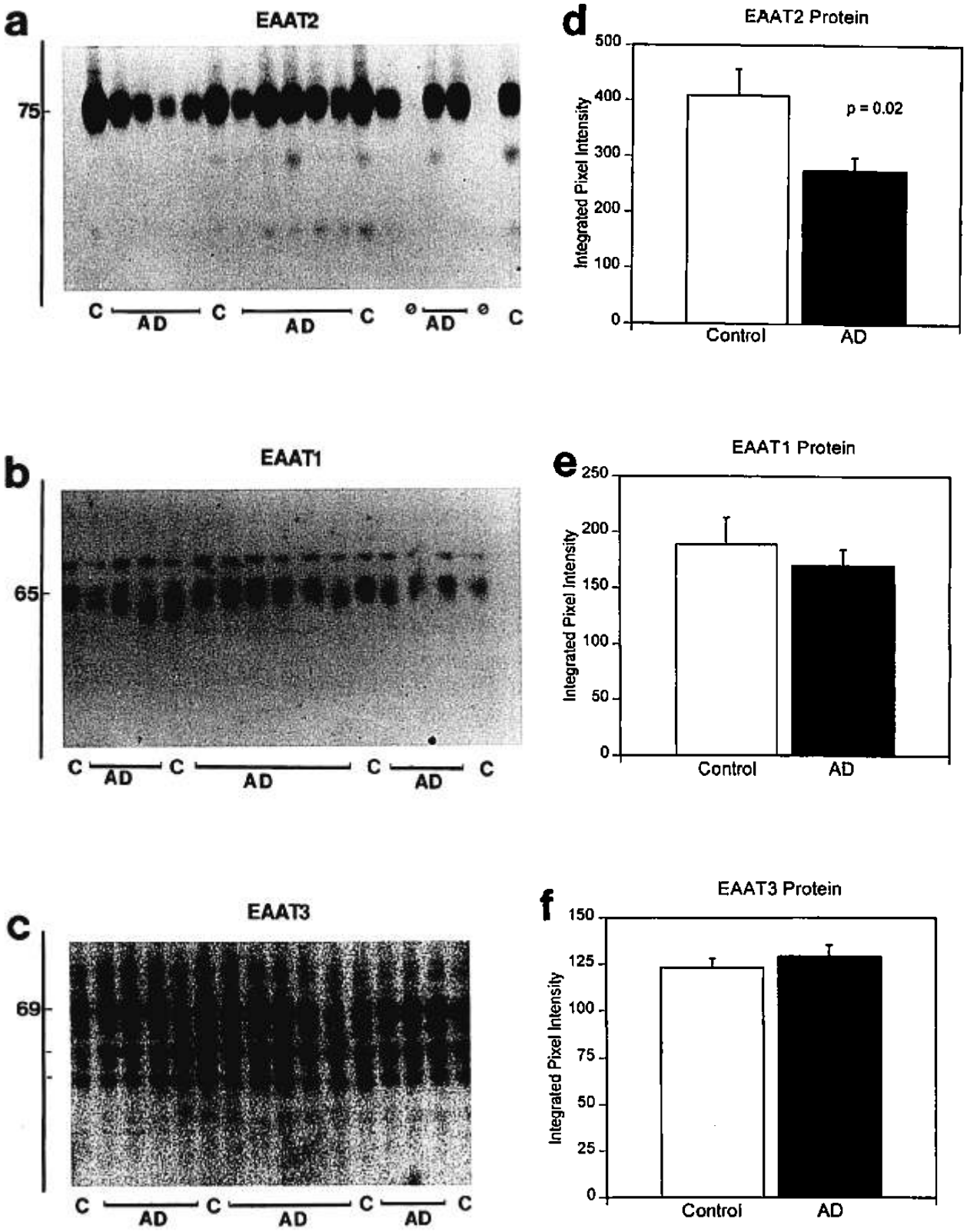

Fig. 2. Levels of GT-IR in frontal cortex by Western blot. The antibody against EAAT2 recognized a major band at an estimated MW of 75 kDa (a), while EAAT1 recognized a major band at 65 kDa (b) and EAAT3 at 69 kDa (c). (d) Compared with controls, AD cases showed a significant 30% decrease in EAAT2 frontal cortex levels. No significant differences in the levels of EAAT1- (e) and EAAT3- (f) IR were observed between AD and control cases.

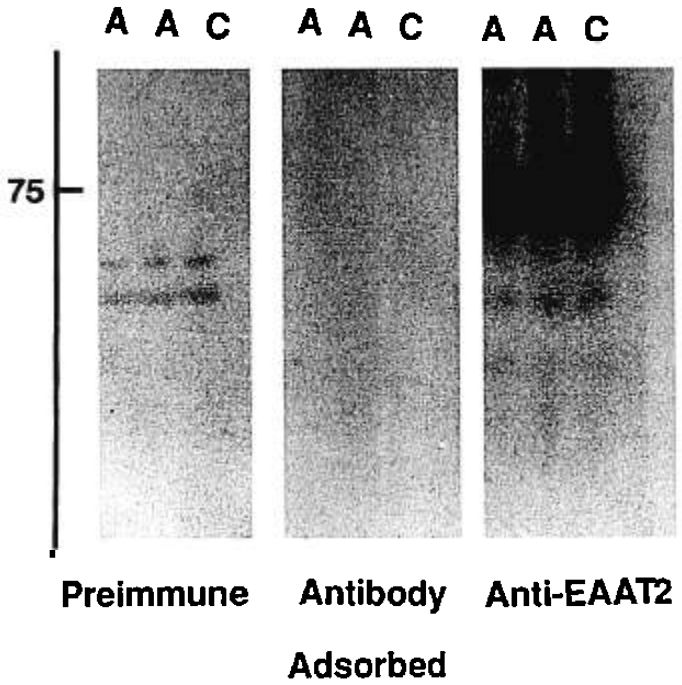

Fig. 3. Specificity of the antibody against EAAT2. In control experiments, the preimmune serum did not recognize the major specific bands. Also, when the primary antibody was adsorbed with excess peptide, the specific bands were not labeled. A = AD; C = Control.

Correlations between GT and APP Expression

Overall levels of APP-IR were assessed by Western blot with the monoclonal antibody 8E5. This antibody recognized a triplet band at an estimated MW of 110-120 kDa (not shown). Levels of L-[^{3}H]aspartate binding in the frontal cortex were directly correlated with levels of APP-IR ($r = 0.6$, $n = 13$, $p = 0.0029$) (Fig. 7a) by Western blot. No significant correlations were observed between APP-IR by Western blot and mRNA levels for EAAT1, EAAT2 and EAAT3.

Further evaluation of the levels of expression and alternative splicing of APP was performed by RT-PCR. This assay for brain APP mRNAs revealed 3 bands in autoradiography at positions 628 bp, 796 bp and 853 bp, corresponding to APP695, APP751 and APP770 mRNAs, respectively (not shown). Linear regression analysis showed that levels of EAAT1 mRNA were inversely correlated with APP695 ($r = -0.629$, $n = 12$, $p = 0.02$) and directly correlated with levels of APP751 ($r = 0.6$, $n = 12$, $p = 0.04$) and APP770 ($r = 0.692$, $n = 12$, $p = 0.012$) mRNA levels. EAAT2-IR were inversely correlated with APP770 mRNA ($r = -0.63$, $n = 13$, $p = 0.02$) (Fig. 7b) and showed a trend toward a direct correlation with APP695 ($r = 0.4$, $n = 13$, $p = 0.18$) and an inverse correlation with levels of APP751 ($r = -0.3$, $n = 13$, $p = 0.30$) mRNA. In addition, L-[^{3}H]aspartate binding levels were directly correlated with APP695 ($r = 0.635$, $n = 12$, $p = 0.02$) and inversely correlated with levels of APP751 ($r = -0.643$, $n = 12$, $p = 0.02$) and APP770 ($r = -0.6$, $n = 12$, $p = 0.04$) mRNA levels (Fig. 7c).

DISCUSSION

Previous studies have shown that in AD the activity of the glutamate/aspartate uptake system is decreased in neocortical areas involved in cognitive functioning (12–15, 36, 37). However, it was not determined which GT was selectively affected in AD. The present study showed that of the 3 different GTs analyzed, EAAT2 was the most significantly affected in AD. Decreased EAAT2 protein expression in AD was associated with decreased GT activity as reflected by D-[^{3}H]aspartate binding. Decreased EAAT2-IR and activity in frontal cortex of AD cases might be associated with the extent of the neurodegenerative process and/or with decreased number of cells containing EAAT2. Since EAAT2 is mainly produced by astroglial cells (8), and since there is significant astrogliosis in AD (38), it is unlikely that the lower level of IR and activity are the result of fewer cells producing EAAT2, supporting the possibility that decreased EAAT2 is associated with the extent of the neurodegenerative process. Recent studies have shown that levels of brain spectrin degradation products were correlated with a decrease in the levels of D- and L- [^{3}H]aspartate binding (15). This indicates that altered functioning of GT in AD might lead to degeneration because calpain I-mediated proteolysis of brain spectrin (39, 40) has been proposed as an indicator of the Ca^{2+}-activated, excitatory amino acid–induced neuronal death (41, 42).

Lower levels of EAAT2-IR and activity in AD might be the result of impaired protein synthesis, increased protein degradation, decreased mRNA survival, and/or decreased mRNA synthesis and post-transcriptional modifications. Since the levels of GT mRNA expression were not altered in AD, this suggests that lower levels of EAAT2-IR are not the result of transcriptional alterations. In fact, EAAT2 protein levels were inversely correlated with EAAT2 mRNA levels, supporting the possibility that alterations in GT expression in AD occur as a result of a disturbance at the post-transcriptional level and that a feedback mechanism might stimulate a relative increase in mRNA levels to compensate for the decreased protein expression and binding. In ALS there also is decreased EAAT2-IR with preserved levels of mRNA within the motor cortex and spinal cord (43). Taken together this indicates that altered functioning of selective GTs might be related to post-transcriptional modifications.

Regarding regulatory post-transcriptional modifications, recent studies have shown that GT functioning is modulated by protein kinase C–mediated phosphorylation of a serine residue located in the loop connecting putative transmembrane helices 2 and 3 (44). Activation of GT was due to an increased phosphorylation of this site. Therefore,

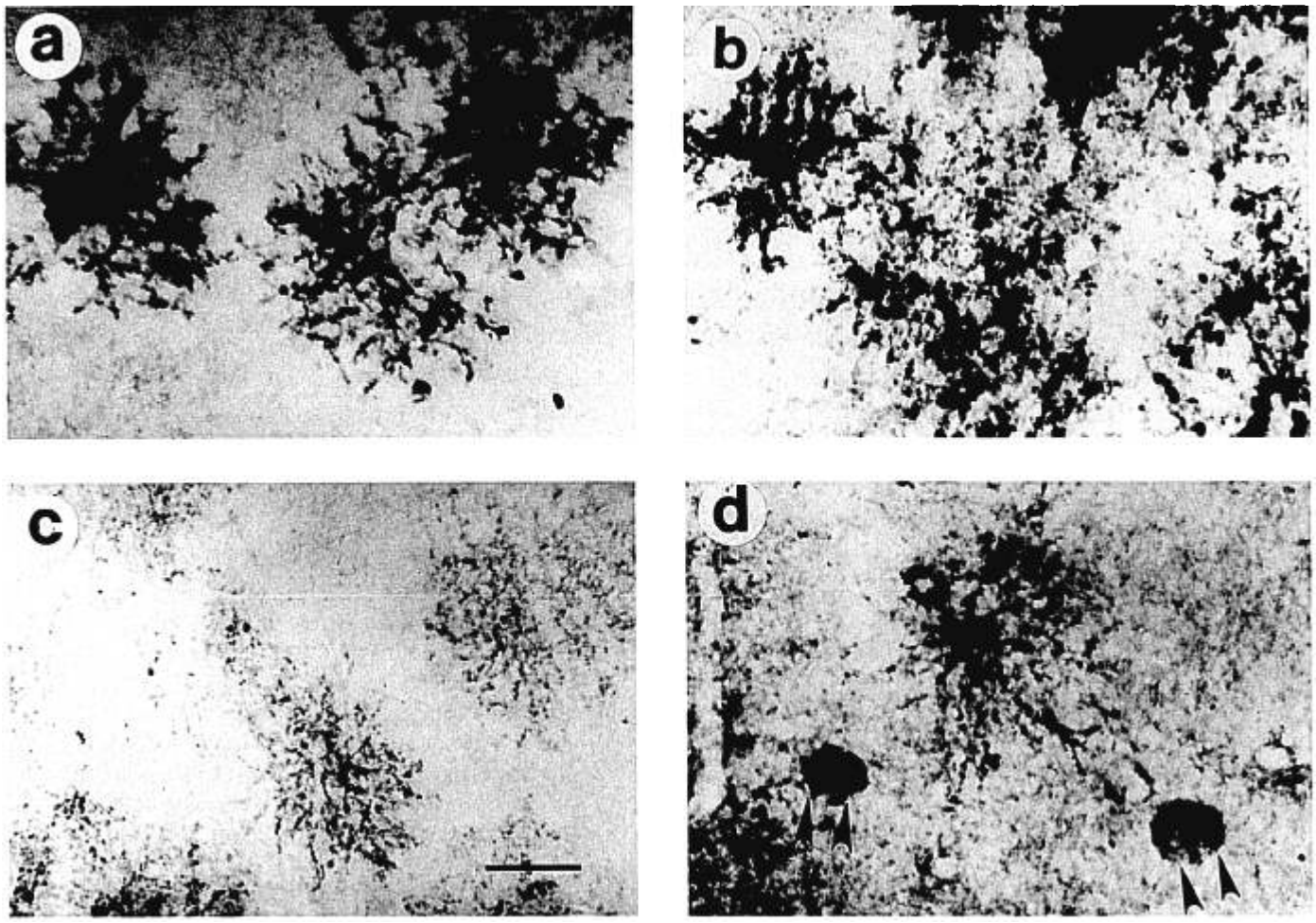

Fig. 4. Patterns of GT-like IR in the brain. In control cases, EAAT2-IR was associated mainly with glial cells with abundant processes in the frontal cortex (a) and hippocampus (b). In AD cases, EAAT2-IR was also associated with glial cells in the neocortex (c) and hippocampus (d). These cells displayed a decrease in the intensity of immunolabeling when compared with controls. In addition, in AD cases, plaques were immunolabeled by the anti-EAAT2 antibody (arrowheads).

factors involved in regulating GT functioning and/or phosphorylation might be responsible for the alterations in GT observed in AD. For the present study we proposed that altered functioning of GT in AD might be associated with abnormal APP expression. This hypothesis is based on recent studies showing that APP exerts neuroprotective properties against acute and chronic excitotoxicity (17, 45), probably by regulating the functioning of GTs (22). Supporting the possibility that altered APP expression might result in abnormal GT functioning, the present study showed that EAAT2-IR was inversely correlated with APP770 mRNA. Furthermore, GT activity was directly correlated with APP695 mRNA and APP IR and inversely correlated with APP751/770 mRNA levels. These findings indicate that the various isoforms of APP might be involved in regulating GT functioning. In AD, the ratio among the various isoforms of APP is shifted toward the longer forms, and APP processing is shifted toward increased production of amyloidogenic fragments (for review see [23]). This suggests that in AD increased production of amyloidogenic fragments and/or generation of secreted APPβ might interfere with GT function. Supporting this possibility, previous studies have shown that a synthetic peptide homologous to amyloid β protein (25–35) blocks the functioning of GT in vitro (46). This amyloid β protein fragment has been previously shown to promote neuronal death in vitro (47) and to generate reactive oxygen radicals (46); however, amyloid β protein 1-40 and 1-42 are produced in vivo (48, 49) rather than free amyloid β protein 25-35. The effects of these amyloidogenic fragments of APP on GTs are not currently known. In their study, Harris et al (46) propose 3 potential mechanisms for the inhibition of glutamate uptake: (a) inhibition of the Na^+, K^+-ATPase, (b) direct oxidative damage to the GT molecule, and (c) membrane perturbations by lipid peroxidation. Of these possibilities, Harris et al suggest that direct inhibition of the GT is the most likely. Although the direct effect of amyloid β protein might play

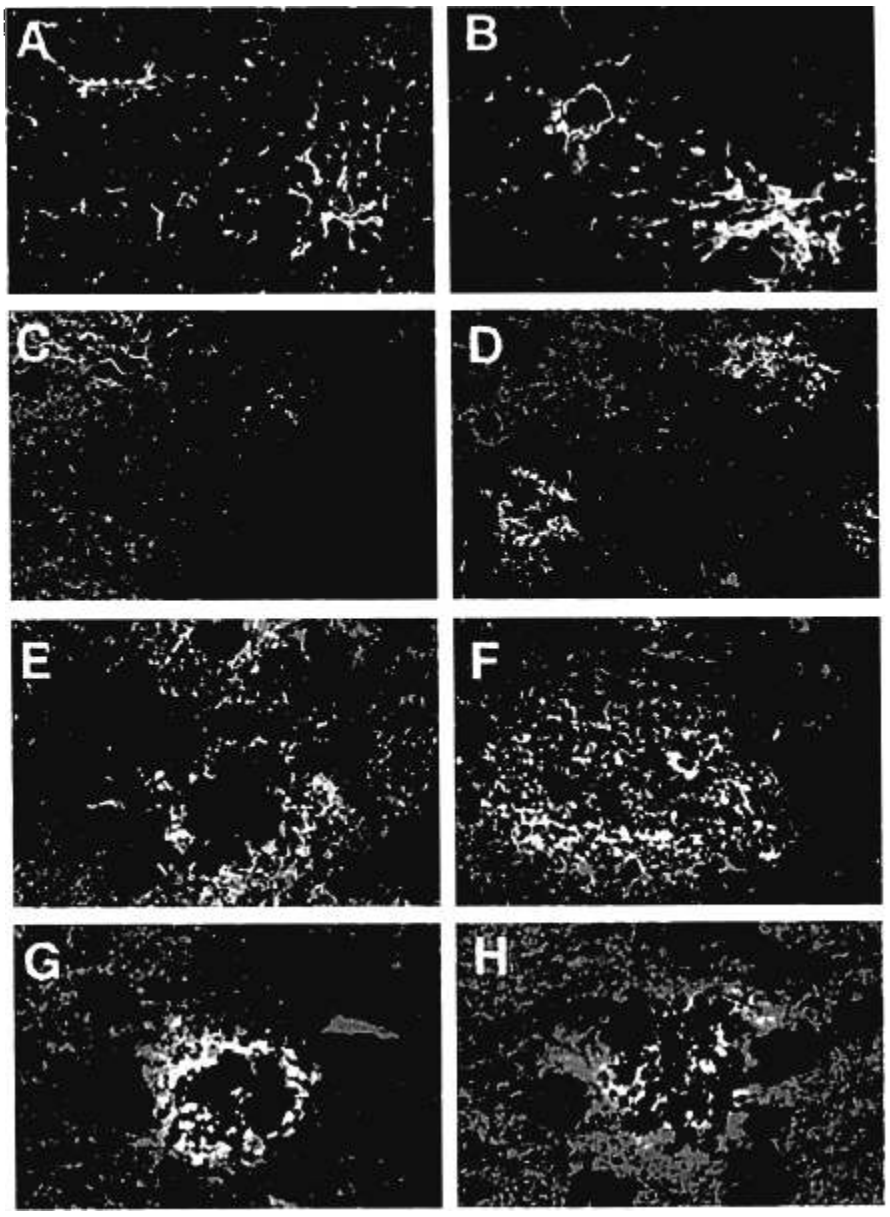

Fig. 5. Studies of cellular distribution of GT-like IR in AD. Sections were double-immunolabeled with antibodies against EAAT2 (FITC, green) and either GFAP or amyloid β protein (Texas red) and imaged with the laser scanning confocal microscope. EAAT2-immunoreactive cells in the neocortex often displayed anti-GFAP-IR (a). EAAT2-IR was more prominent in the periphery of the glial cell bodies and their processes (b). EAAT2-IR was colocalized with GFAP-immunoreactive glial cells surrounding amyloid plaques (c, d). EAAT2-IR was also associated with a fine meshwork of astroglial processes embedded in the diffuse amyloid plaques (e, f) and to a lesser extent in the mature amyloid plaques (g, h).

an important role in blocking EAAT2 functioning in vivo in AD, it is unlikely that this is the only mechanism involved since, as the present study showed, the greater proportion of astrocytes (that produce EAAT2) are not in close contact with dense amyloid deposits, but in fact are diffusely scattered throughout the neuropil, particularly in those regions where neuronal and synaptic loss is more pronounced (50). Therefore, malfunctioning of GTs in AD might be related not only to amyloid β protein production, but also to generation of sAPP fragments that might not be fully capable of activating GTs. In this regard, a recent study showed that sAPPβ is less potent than sAPPα in protecting neurons against excitotoxicity and metabolic insults (51). More direct evidence to support this hypothesis will also require detailed in vivo studies where determination of GT function and expression is

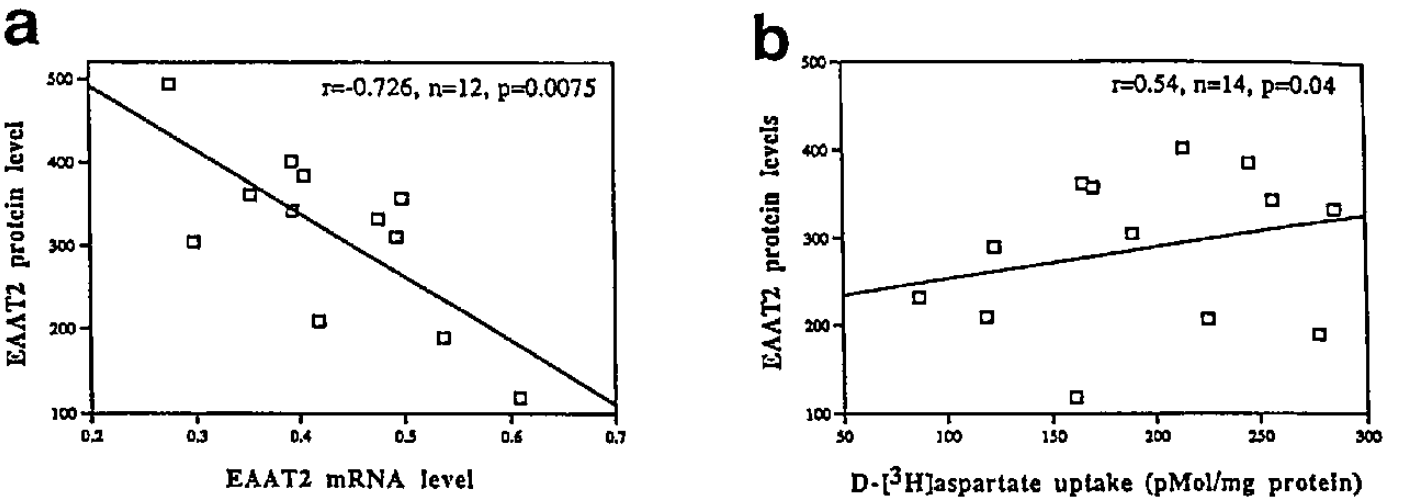

Fig. 6. Correlations between GT expression and activity. Linear regression analysis showed (a) that there was a strong inverse correlation between EAAT2 mRNA and IR and (b) that D-[3H]aspartate uptake and EAAT2-IR were directly correlated.

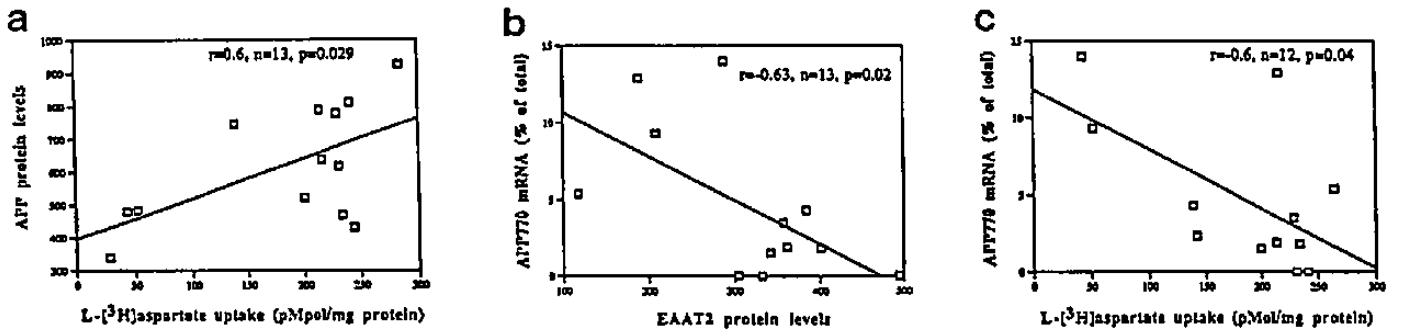

Fig. 7. Correlations of GT with APP expression. Linear regression analysis showed (a) that levels of L-[3H]aspartate uptake in the frontal cortex were directly correlated with levels of APP-IR by Western blot, (b) that EAAT2-IR was inversely correlated with APP770 mRNA, and (c) that L-[3H]aspartate uptake levels were directly correlated with APP770 mRNA.

performed in transgenic mice that express sAPPα or sAPPβ.

In conclusion, the present study supports the notion that astroglial EAAT2 is affected in the AD frontal cortex and that abnormal functioning and/or processing of APP might play an important role in this process. Taken together, these results support the possibility that decreased activity of GTs in AD is associated with increased excitotoxicity and neurodegeneration.

REFERENCES

1. Greenamyre JT, Porter RHP. Anatomy and physiology of glutamate in the CNS. Neurology 1994;44(suppl):S7–13
2. Kanai Y, Smith CP, Hediger MA. The elusive transporters with a high affinity for glutamate. Trends Neurosci 1993;16:359–65
3. Balcar VJ, Li Y. Heterogeneity of high affinity uptake of L-glutamate and L-aspartate in the mammalian central nervous system. Life Sci 1992;51:1467–78
4. Storck T, Schulte S, Hofman K, Stoffel W. Structure, expression, and functional analysis of a Na+-dependent glutamate/aspartate transporter from rat brain. Proc Natl Acad Sci USA 1992;89: 10955–59
5. Pines G, Danbolt NC, Bjoras M, Zhang Y, Bendahan A, Eide L, Koepsell H, Storm-Mathisen J, Seeberg E, Kanner BI. Cloning and expression of a rat brain L-glutamate transporter. Nature 1992; 360:464–67
6. Kanai Y, Hediger MA. Primary structure and functional characterization of a high-affinity glutamate transporter. Nature 1992;360: 467–71
7. Kanai Y, Nussberger S, Romero MF, Boron WF, Hebert SC, Hediger MA. Electrogenic properties of the epithelial and neuronal high affinity glutamate transporter. J Biol Chem 1995;270:16561–68
8. Rothstein JD, Martin L, Levey AI, Dykes-Hoberg M, Kuncl RW. Localization of neuronal and glial glutamate transporters. Neuron 1994;13:713–25
9. Rothstein JD, Jin L, Dykes-Hoberg M, Kuncl RW. Chronic inhibition of glutamate uptake produces a model of slow neurotoxicity. Proc Natl Acad Sci USA 1993;90:6591–95
10. Rothstein JD, Dykes-Hoberg M, Pardo CA, et al. Knockout of glutamate transporters reveals a major role for astroglial transport in excitotoxicity and clearance of glutamate. Neuron 1996;16:675–86
11. Rothstein JD, Van Kammen M, Levey AI, Martin LJ, Kuncl RW. Selective loss of glial glutamate trasporter GLT-1 in amyotrophic lateral sclerosis. Ann Neurol 1995;38:73–84
12. Scott HL, Tannenberg AEG, Dodd PR. Variant forms of neuronal glutamate trasporter sites in Alzheimer's disease cerebral cortex. J Neurochem 1995;64:2193–2202

13. Cowburn R, Hardy J, Roberts P, Briggs R. Presynaptic and postsynaptic glutamatergic function in Alzheimer's disease. Neurosci Lett 1988;86:109–13
14. Cowburn RF, Hardy JA, Roberts PJ. Glutamatergic neurotransmission in Alzheimer's disease. Biochem Soc Trans 1990;18:390–92
15. Masliah E, Alford M, Salmon D, DeTeresa R, Mallory M, Hansen L. Deficient glutamate transporter activity in Alzheimer's disease is associated with accumulation of brain spectrin degradation products and neurodegeneration. Ann Neurol 1997;40:759–66
16. Mattson MP, Cheng B, Culwell AR, Esch FS, Lieberburg I, Rydel RE. Evidence for excitoprotective and intraneuronal calcium-regulating roles for secreted forms of the ß-amyloid precursor protein. Neuron 1993;10:243–54
17. Mucke L, Abraham CR, Ruppe MD, Rockenstein EM, Toggas SM, Alford M, Masliah E. Protection against HIV-1 gp120-induced brain damage by neuronal overexpression of human amyloid precursor protein (hAPP). J Exp Med 1995;181:1551–56
18. Masliah E. Mechanisms of synaptic dysfunction in Alzheimer's disease. Histol Histopathol 1995;10:509–19
19. Mattson MP, Cheng B, Smith-Swintosky VL. Mechanisms of neurotrophic factor protection against calcium- and free radical-mediated excitotoxic injury: Implications for treating neurodegenerative disorders. Exp Neurol 1993;124:89–95
20. Mattson MP, Tomaselli KJ, Rydel RE. Calcium-destabilizing and neurodegenerative effects of aggregated β-amyloid peptide are attenuated by basic FGF. Brain Res 1993;621:35–49
21. Furukawa K, Barger SW, Blalock E, Mattson MP. Activation of K+ channels and suppression of neural activity by secreted β-amyloid precursor protein. Nature 1996;379:74–78
22. Masliah E, Raber J, Alford M, Mallory M, Mattson MP, Westland CE, Mucke L. Amyloid protein precursor stimulates excitatory amino acid transport: Possible involvement in neuroprotective in vivo functions. J Biol Chem 1997. Forthcoming.
23. Rockenstein EM, McConlogue L, Tan H, Power M, Masliah E, Mucke L. Levels and alternative splicing of amyloid β protein precursor (APP) transcripts in brains of APP transgenic mice and humans with Alzheimer's disease. J Biol Chem 1995;270:28257–67
24. Terry RD, Peck A, DeTeresa R, Schechter R, Horoupian DS. Some morphometric aspects of the brain in senile dementia of the Alzheimer type. Ann Neurol 1981;10:184–92
25. Wiedenmann B, Franke WW. Identification and localization of synaptophysin, an integral membrane glycoprotein of Mr 38,000 characteristic of presynaptic vesicles. Cell 1985;41:1017–28
26. Masliah E, Terry RD, Alford M, DeTeresa RM, Hansen LA. Cortical and subcortical patterns of synaptophysin-like immunoreactivity in Alzheimer disease. Am J Pathol 1991;138:235–46
27. Mucke L, Masliah E, Johnson WB, et al. Synaptotrophic effects of human amyloid β protein precursors in the cortex of transgenic mice. Brain Res 1994;666:151–67
28. Alford MF, Masliah E, Hansen LA, Terry RD. A simple dot-immunobinding assay for the quantification of synaptophysin-like immunoreactivity in human brain. J Histochem Cytochem 1994;42: 283–87
29. Lowry OH, Rosenbrough NJ, Farr AL, Randall RJ. Protein measurement with Folin phenol reagent. Biol Chem 1951;193:265–72
30. Buxbaum JD, Gandy SE, Cicchetti P, et al. Processing of Alzheimer β /A4 amyloid precursor protein: Modulation by agents that regulate protein phosphorylation. Proc Natl Acad Sci USA 1990;87: 6003–36
31. Masliah E, Mallory M, Hansen L, DeTeresa R, Alford M, Terry R. Synaptic and neuritic alterations during the progression of Alzheimer's disease. Neurosci Lett 1994;174:67–72
32. Masliah E, Fagan AM, Terry RD, DeTeresa R, Mallory M, Gage FH. Reactive synaptogenesis assessed by synaptophysin immunoreactivity is associated with GAP-43 in the dentate gyrus of the adult rat. Exp Neurol 1991;113:131–42
33. Toggas SM, Masliah E, Rockenstein EM, Mucke L. Central nervous system damage produced by expression of the HIV-1 coat protein gp120 in transgenic mice. Nature 1994;367:188–93
34. Iwai A, Masliah E, Sundsmo MP, DeTeresa R, Mallory M, Salmon DP, Saitoh T. The synaptic protein NACP is abnormally expressed during the progression of Alzheimer's disease. Brain Res 1996;720: 230–34
35. Cross AJ, Skan WJ, Slater P. The association of [³H]d-aspartate binding and high-affinity glutamate uptake in the human brain. Neurosci Lett 1986;63:121–24
36. Simpson MDC, Slater P, Cross AJ, Mann DMA, Royston MC, Deakin JFW, Reynolds GP. Reduced D-[³H]asparate binding in Down's syndrome brains. Brain Res 1989;484:273–78
37. Simpson MD, Royston MC, Deakin JF, Cross AJ, Mann DM, Slater P. Regional changes in [³H]D-aspartate and [³H]TCP binding sites in Alzheimer's disease brains. Brain Res 1988;462:76–82
38. Dickson DW, Farlo J, Davies P, Crystal H, Fuld P, Yen SC. Alzheimer disease. A double immunohistochemical study of senile plaques. Am J Pathol 1988;132:86–101
39. Lynch G, Baudry M. Brain spectrin, calpain and long term changes in synaptic efficacy. Brain Res Bull 1987;18:809–15
40. Seubert P, Ivy G, Larson J, Lee J, Shahi K, Baudry M, Lynch G. Lesions of entorhinal cortex produce a calpain-mediated degradation of brain spectrin in dentate gyrus. I. Biochemical studies. Brain Res 1988;459:226–32
41. Lowy MT, Wittwnberg L, Yamamoto BK. Effect of acute stress on hippocampal glutamate levels and spectrin proteolysis in young and aged rats. J Neurochem 1995;65:268–74
42. Broroson JR, Marcuccilli CJ, Miller RJ. Delayed antagonism of calpain reduces excitotoxicity in cultured neurons. Stroke 1995; 26:1259–67
43. Bristol LA, Rothstein JD. Glutamate trasporter gene expression in amyotrophic lateral sclerosis motor cortex. Ann Neurol 1996;39: 676–79
44. Casado M, Bendahan A, Zafra F, Danbolt NC, Aragon C, Gimenez C, Kanner BI. Phosphorylation and modulation of brain glutamate transporters by protein kinase C. J Biol Chem 1993;268:27313–17
45. Masliah E, Westland CE, Abraham CR, Mallory M, Veinbergs I, Rockenstein EM, Mucke L. Amyloid precursor protein protects neurons of transgenic mice against acute and chronic excitotoxic injuries *in vivo*. Neurosci 1997;78:135–41
46. Harris ME, Wang Y, Pedigo NWJr, Hensley K, Butterfield DA, Carney JM. Amyloid β peptide (25-35) inhibits Na^+- dependent glutamate uptake in rat hippocampal astrocyte cultures. J Neurochem 1996;67:277–86
47. Weiss JH, Pike CJ, Cotman CW. Ca2+ channel blockers attenuate beta-amyloid peptide toxicity to cortical neurons in culture. J Neurochem 1994;62:372–75
48. Selkoe DJ. Physiological production of the β-amyloid protein and the mechanisms of Alzheimer's disease. Trends Neurosci 1993;16: 403–9
49. Seubert P, Vigo-Pelfrey C, Esch F, et al. Isolation and quantification of soluble Alzheimer's β-peptide from biological fluids. Nature 1992;359:325–27
50. Saitoh T, Kang D, Mallory M, DeTeresa R, Masliah E. Glial cells in Alzheimer's disease: Preferential effect of APOE risk on scattered microglia. Gerontology 1997;43:109–18
51. Furukawa K, Sopher BL, Rydel RE, Begley JG, Pham DG, Martin GM, Fox M, Mattson MP. Increased activity regulating and neuroprotective efficacy of α-secretase-derived secreted amyloid precursor protein conferred by a c-terminal heparin-binding domain. J Neurochem 1996;67:1882–92

Received March 18, 1997
Revision received May 27, 1997
Accepted May 29, 1997